High Harmonic Forces and Predicted Vibrations from Forced In-line and Cross-flow Cylinder Motions

Proceedings of the Eighteenth (2008) International Offshore and Polar Engineering Conference
Vancouver, BC, Canada, July 6-11, 2008

ISBN 978-1-880653-70-8 (Set); ISBN 1-880653-68-0 (Set)

High Harmonic Forces and Predicted Vibrations from Forced In-line and Cross-flow Cylinder Motions

J.M. Dahl, F.S. Hover, M.S. Triantafyllou
Department of Mechanical Engineering, Massachusetts Institute of Technology
Cambridge, MA

ABSTRACT

String-like ocean structures, such as deep water marine risers are susceptible to a condition of dual lock-in, where both the in-line and transverse natural frequencies are excited due to vortex shedding in the wake. This type of excitation can result in dominant, large amplitude third harmonic forces in the cross-flow direction that do not exist in conditions allowing only cross-flow motion. Forced motions of a rigid cylinder in both the in-line and cross-flow directions are performed to obtain coefficients defining the magnitude of third harmonic lift forces for given cylinder motions. In-line motion amplitude, cross-flow amplitude, phase between in-line and cross-flow motion, and reduced velocity are varied, producing a four-dimensional matrix of data points, at a Reynolds number of 8800. In free vibrations, variation of the effective added mass drives the system to specific steady-state oscillations, under lock-in conditions. These free vibration steady-state oscillations are successfully predicted with the new forced oscillation data set, using the simplifying assumption that lock-in occurs in both the in-line and cross-flow directions, and the necessary assumption that the normalized average power over one cycle must be zero for a free vibration. The new data set and our procedure will allow a more accurate strip-theory approach to marine riser VIV analysis and design.

KEY WORDS: VIV; vortex-induced vibration; 2 DOF; forced vibration

INTRODUCTION

As the demand for natural resources drives ocean structures, such as marine risers, to deep water, the necessity for an accurate understanding of the physics of the combined in-line and cross-flow oscillation of these structures due to vortex shedding becomes apparent. The fundamental problem of vortex-induced vibrations and a number of studies on the topic are discussed in various comprehensive reviews (Sarpkaya, 1979, 2004; Bearman, 1984; Williamson and Govardhan, 2004).

Ocean structures such as risers and cables typically have comparable structural mass compared with the displaced mass of fluid (mass ratio, m*~ 2) and very low structural damping (damping coefficient, $\zeta <$ 0.01). In modeled riser motions, such as in the case of an elastically mounted circular cylinder, it has been shown that low structural damping and mass ratio can lead to large resonant amplitudes and increased bandwidth of the resonant region of excitation (Khalak and Williamson, 1996).

Very long, flexible risers exhibit structural characteristics similar to long beams or strings depending on the application. If one considers a long cylindrical structure to be similar to a beam under tension, it possesses a countable set of natural frequencies and modes in the in-line and transverse directions, as in equation 1, where n denotes mode number, E denotes modulus of elasticity, I is the area moment of inertia, L is the beam length, M is the mass per unit length, and T is the axial tension force in the beam.

$$f_{beam} = \sqrt{\frac{n^4 \pi^2 EI}{4L^4 M} + \frac{n^2 T}{4L^2 M}} \quad (1)$$

The first term of equation 1 is the natural frequency of a particular mode for a bending dominated system, such as a beam, with simply supported end conditions. The second term of the equation is the natural frequency of a particular mode for a string in tension. Depending on the ratio of the tension to bending stiffness, the natural frequency of the n^{th} mode lies between n (string) and n^2 (beam) times the fundamental natural frequency of the system.

Vortex shedding in the wake of a fixed circular cylinder in a free stream is characterized by the Kàrmàn vortex street, where vortices shed periodically in the wake of the cylinder at the Strouhal frequency. For flexible cylinders or elastically mounted rigid cylinders, the wake behind the cylinder is characterized by the periodic shedding of vortices or groups of vortices, which similarly cause periodic forcing on the cylinder; forces exerted on the cylinder are a function of this periodic vortex shedding. The in-line excitation force from vortex shedding has a frequency twice the cross-flow forcing frequency as a result of the shedding process.

A condition of dual resonance may occur when the cross-flow natural frequency of the structure is equal, or at least close to the frequency of vortex shedding, f_s, and the in-line natural frequency is equal to twice the shedding frequency, i.e. $f_{ny} \sim f_s$ and $f_{nx}/f_{ny} = 2$. This condition is illustrated in Fig. 1, where the first mode of the tensioned beam is excited in the cross-flow (y) direction and the second mode is excited in the in-line (x) direction.

In a beam, the ratio f_{nx}/f_{ny} can rarely reach a value close to 2 because of the n^2 relation between beam natural frequencies. Cross-flow motion will resonate from fluid excitation in this case, while in-line motion is non-resonant. Shallow water structures are typically bending dominated systems, bearing characteristics closer to a beam than a string. These characteristics result in typical excitation of beam modes under the

condition $f_{nx}/f_{ny} \sim 1$, meaning that dual resonance is not possible. In deep water however, dual resonance of very long structures is nearly inevitable as the number of modes increase and the structure appears string-like. A condition of $f_{nx}/f_{ny} = 2$ is more likely to appear for a very long string. Previous studies have investigated this relation between in-line and transverse natural frequencies by varying this ratio for an elastically mounted cylinder which is allowed to move in combined cross-flow and in-line motions (Dahl et al, 2006; Jauvtis and Williamson, 2004; Sarpkaya, 1995).

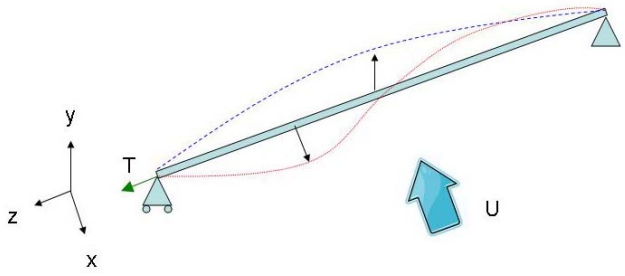

Fig. 1: Schematic of a tensioned beam with the first mode excited in the cross-flow direction and the second mode excited in the in-line direction, $f_{nx}/f_{ny} = 2$.

Sarpkaya (1995) showed that when a cylinder freely vibrates in combined in-line and cross-flow motions, the amplitudes of motion are larger than those observed for a cylinder restricted to cross-flow motion only. In a condition of dual resonance, where the cylinder was set to have $f_{nx}/f_{ny} = 2$, two peaks in the amplitude response of the cylinder were observed, one at reduced velocity near 5, where cross-flow only oscillations peak, and one at a higher reduced velocity, near 7. Jauvtis and Williamson (2004) found that a cylinder with $f_{nx}/f_{ny} = 1$, with low mass-damping, is excited with very large cross-flow amplitudes of motion, in excess of $A_y/D = 1.5$. These large cross-flow motions result in the formation of vortex triplets that form every half cycle of motion. Lift forces were found to have a third harmonic component and this third harmonic was attributed to the presence of vortex triplets. Similar large amplitude oscillations of a cylinder allowed to move in cross-flow and in-line motion were observed by Dahl et al (2006) for intermediate natural frequency ratios between 1 and 2. At natural frequency ratios near 2, Dahl et al (2007) found that third harmonic force components observed in lift were very large, even dominant, when compared with the first harmonic component of lift. Dominant third harmonic lift components were associated with particular cylinder motions such as when the cylinder moves in a figure eight shape with downstream motion as it crosses the centerline of the figure eight. Large third harmonics have the potential for drastically decreasing fatigue life of marine risers through increased material stresses and increased cyclical loading of the structure.

Typical force models concerned with vortex-induced vibrations only consider forces associated with the cross-flow oscillation of the structure. In these models, forces are assumed to occur with the fundamental frequency of vortex shedding. The previously indicated studies show that this assumption is not always true, and forces associated with combined cross-flow and in-line motion can be drastically different than those observed for only cross-flow motions. Since the combined cross-flow and in-line motion of a circular cylinder is commonly observed in marine risers, this type of motion must be taken into account for predicting motions of the riser and forces exerted on the riser.

The purpose of this study was to characterize the forces associated with cross-flow and in-line motions of a circular cylinder over a wide range of possible riser motions. In this study, a circular cylinder is forced to move in the cross-flow and in-line direction while moving through a steady free stream of fluid. The cylinder is forced at a variety of in-line amplitudes, cross-flow amplitudes, phases between in-line and cross-flow motions, and reduced velocity, while fluid forces in lift and drag are measured. The region where potential free vibrations occur, as determined by the average power over one cycle of cross-flow motion, is shown to be very large, consisting of a large number of motion parameter combinations. The particular structural characteristics of the elastically mounted, rigid cylinder are shown to define the particular motions that the cylinder will have under certain flow conditions. The measurement of fluid forces are used to predict the self-excited motions of an elastically mounted, rigid cylinder, based on simple assumptions about the condition of lock-in. It is found that assuming a condition of dual resonance is sufficient for predicting these cylinder motions.

EXPERIMENTAL PROCEDURE

Experimental Apparatus

Experiments were performed in a small towing tank, 2.4 m long, 0.75 m wide, and 0.7 m deep. Two linear motors, mounted perpendicular to one another, were fixed to a moving carriage that could be towed along the length of the tank at constant speed. The test cylinder, circular in cross section, with a diameter of 38.1 mm and span of 0.6858 m, was cantilevered from the linear motors so the cylinder could be forced to move in the in-line and cross-flow directions. The rigid test cylinder was made from thin-walled aluminum tubing. A six-axis strain gage force sensor was mounted between the linear motor cantilever and the test cylinder in order to measure fluid forces exerted on the cylinder. The natural frequency of the cantilevered cylinder was far from the excitation frequency of fluid forces, minimizing forces due to excitation of the test apparatus natural frequencies. The cylinder mass was determined to three significant digits (0.245 kg) in order to remove test cylinder inertial forces from the force measurement. An extensive six-axis calibration of the force sensor was performed to determine the cross-coupling effects between sensor directions. The short tank length limits the useful (steady state) force coefficient data to between 4 and 10 cycles of motion, depending on the reduced velocity. This limitation results in limited frequency resolution of force measurements.

Test Matrix

The test cylinder is towed at a constant velocity, U, and the linear motors force the cylinder with sinusoidal motions. The particular cross-flow (y) and in-line (x) motions are defined in equations 2 and 3, where.

$$\frac{y(t)}{D} = \frac{A_y}{D}\sin \omega t \quad (2)$$

$$\frac{x(t)}{D} = \frac{A_x}{D}\sin(2\omega t + \theta) \quad (3)$$

The parameters A_y/D and A_x/D define the amplitude of sinusoidal motions, while phase angle, θ, describes the phase between these motions. The phase between in-line and cross-flow motions is a significant parameter as it affects the particular path of motion through the fluid. Jeon and Gharib (2001) found that the phase between in-line and transverse motion could delay the onset of particular vortex shedding patterns in the wake of the cylinder. In a reference frame fixed to the carriage, these three parameters define the shape and path of the cylinder motion as shown in Fig. 2.

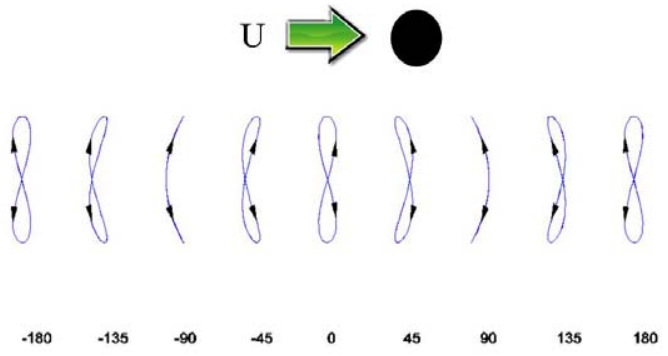

Fig. 2: Schematic of cylinder motions for various phase angles, θ (in degrees). Flow velocity is from left to right.

An additional non-dimensional parameter significant to vortex-induced vibrations is the reduced velocity. This is a comparison of the free stream flow velocity with the cross-flow oscillation velocity. The reduced velocity is defined as in equation 4, where U is the free stream velocity, f is the cross-flow oscillation frequency of the cylinder, and D is the cylinder diameter.

$$V_r = \frac{U}{fD} \tag{4}$$

The motion parameters A_y/D, A_x/D, V_r, and θ were varied to construct a sparse matrix of forced cylinder motions. The cross-flow amplitude, A_y/D, was varied with six values between 0.25 and 1.5 in increments of 0.25. The in-line amplitude, A_x/D, was varied with six values between 0 and 0.75 in increments of 0.15. Phase angle, θ, was varied with eight values between -180 degrees and 135 degrees in increments of 45 degrees (180 degrees is equivalent to -180 degrees). Reduced velocity, V_r, was varied with eight values between 4.5 and 8 in increments of 0.5. This results in a sparse test matrix of 2304 experiments. The ranges of parameters are chosen based on observed free vibrations of elastically mounted rigid cylinders (Jauvtis and Williamson, 2004, Dahl et al, 2007). The intention of this matrix is not to provide a finely detailed representation of forces, but rather to show how forces vary over this limited range of motion parameters, hence a sparse representation of the motions is sufficient along with the limited frequency resolution. The Reynolds number for the experiments shown was 8800.

Force Measurements

Since the combined cross-flow and in-line motion of a cylinder results in large amplitude high harmonic forces in addition to forces occurring near the fundamental frequency of vortex shedding, it is necessary to compensate for these forces in our force representation. For cross-flow motion only, lift forces are typically treated as a single frequency sinusoidal force, with the same form as the cylinder motion, based on an expansion of Morison's equation (Sarpkaya, 1979). Higher harmonics are typically ignored in the expansion since magnitudes are significantly smaller in comparison with forces at the fundamental frequency. It is necessary to include these higher harmonic components when combined in-line and cross-flow motion occurs, since these forces are no longer insignificant. Equations 5 and 6 show the instantaneous lift and drag coefficients accounting for higher harmonic forces. In these equations, C_{L1} denotes the magnitude of the first harmonic portion of lift and φ_1 is the phase shift between the first harmonic portion of force and cross-flow oscillation, y(t). The third harmonic portions of lift coefficient are denoted by the subscript 3. In the drag direction, high harmonics are not significant, hence the instantaneous drag coefficient consists primarily of a mean drag component, C_{MD}, and the fluctuating drag component with subscript 2.

$$C_L(t) = C_{L1}\sin(\omega t + \varphi_1) + C_{L3}\sin(3\omega t + \varphi_3) + \ldots \tag{5}$$

$$C_D(t) = C_{MD} + C_{D2}\sin(2\omega t + \varphi_2) + \ldots \tag{6}$$

Fluid forces associated with vortex induced vibrations will cause excitation of motion or dissipation of motion depending on the flow of power in the system. In a free vibration, the flow of energy fluctuates over the course of one cycle of motion; however, if the cylinder oscillations are repeatable, the net energy into the system calculated over one cycle of motion must be equal to zero in order to conserve energy. In this case, the energy supplied through fluid forcing must balance energy lost due to damping, resulting in a steady-amplitude periodic oscillation.

The free oscillation of a riser is slightly different, since power must balance along the length of the riser, and power flow is not restricted to a two dimensional plane (the rigid cylinder condition). At a particular two dimensional slice of a flexible riser, it is possible for the net power flow to be positive or negative, depending on the particular motions of the cylinder. In forced vibrations, it is relevant to then consider an average power coefficient, characterizing the flow of power over one cycle of cross-flow motion. The average power over one cycle of motion is defined as the integral in time over one cycle of motion of the total force times the velocity. The power is normalized to produce an average power coefficient, C_{ap}, as in equation 7, where L is the fluctuating lift force, D_f is the fluctuating drag force, T is the period of one cross-flow oscillation, ρ is the density of the fluid, U is the free stream velocity, D is the cylinder diameter, and S is the cylinder span.

$$C_{ap} = \frac{\frac{1}{T}\int_T (L\cdot\dot{y} + D_f\cdot\dot{x})dt}{\frac{1}{2}\rho U^3 DS} \tag{7}$$

The free vibration of an elastically mounted rigid cylinder typically occurs with periodic sinusoidal motions similar to those described by equations 2 and 3. Although forcing in the direction of lift may occur with a large third harmonic component, large amplitude third harmonic excitation of structural motions is typically not seen. In this case, excitation of the structure must occur completely as a function of first harmonic excitation forces; third harmonic forces do not contribute to the excitation of the structure at the first harmonic since third harmonic sinusoids are orthogonal to all first harmonic sinusoids.

Since the third harmonic force does not contribute to structural excitation, we can define the effective added mass associated with cross-flow motion based purely on first harmonic forces in phase with cross-flow acceleration of the body. Similarly, effective added mass in the in-line direction is defined as a function of forces in phase with acceleration of the body in the in-line direction. This representation of added mass forces is consistent with the decomposition of fluid forces discussed by Sarpkaya (1979) and Bearman (1984). The non-dimensional added mass coefficients for cross flow motion, C_{my}, and in-line motion, C_{mx}, are given in equations 8 and 9. All variables are

equivalent to those in the force and motion equations above.

$$C_{my} = \frac{-2U^2 C_{L1} \cos\varphi_1}{\pi A_y D \omega^2} \quad (8)$$

$$C_{mx} = \frac{-2U^2 C_{D2} \cos\varphi_2}{\pi A_x D (2\omega)^2} \quad (9)$$

The effective added mass is a different value than the ideal added mass of a cylinder as calculated from potential flow. The effective added mass is an equivalent mass associated with all fluid forces in phase with the acceleration of the body. In that sense, effective added mass can be a function of both acceleration of fluid with the body and forces caused by vortex shedding in the wake of the cylinder. The effective added mass coefficients given above are equivalent to an effective added mass normalized by the displaced volume of fluid by the cylinder.

OBSERVATIONS FROM FORCED VIBRATIONS

Visualizing the Test Matrix

Since the test matrix consists of four varied parameters, it is difficult to show how force parameters vary as a function of all four motion parameters (in-line motion, cross-flow motion, phase between in-line and cross-flow motion, and reduced velocity). In order to simplify the parameter space, either phase or reduced velocity is held constant to create a three dimensional parameter space. Within this three dimensional space, force coefficients or derived values are known at given points within the three dimensional space, and iso-surfaces of force values can be drawn to indicate how forces vary as a function of in-line motion, cross-flow motion, and reduced velocity or phase between motions.

Average Power

The region over which the average power coefficient, C_{ap}, is zero, determines the theoretical region over which a free vibration with zero damping will occur. Figs. 3-6 show surfaces of zero average power within a parameter space defined by in-line motion, cross-flow motion, and reduced velocity. For each surface that is shown, the phase between motions is held constant and numerous surfaces are drawn in color to signify how these surfaces change with phase. Surfaces of average power are similar to analyzing forces in phase with velocity, except the average power accounts for both in-line and cross-flow motions of the cylinder.

Figs. 3 and 4 show some of the points observed from the experiments of Jauvtis and Williamson (2004) that occur along the upper and super upper branches of their amplitude curves plotted along with the surfaces drawn from the present study forced vibrations. The points from Jauvtis and Williamson are color coded according to the same surface color with the closest phase within 45 degrees. One can see that the particular points from Jauvtis and Williamson (2004) closely follow the boundary region formed by the forced vibration surfaces, indicating that the surfaces are a relatively good estimation of the free vibration motions. The highest amplitudes observed by Jauvtis and Williamson (2004) begin to diverge from the surfaces of the present study since these amplitudes begin to exceed the region of the forced vibration test matrix. It is important to note that the conditions of the experiments of Jauvtis and Williamson (2004) were such that the in-line structural mass was equivalent to the cross-flow structural mass and the in-line natural frequency was equal to the cross-flow natural frequency.

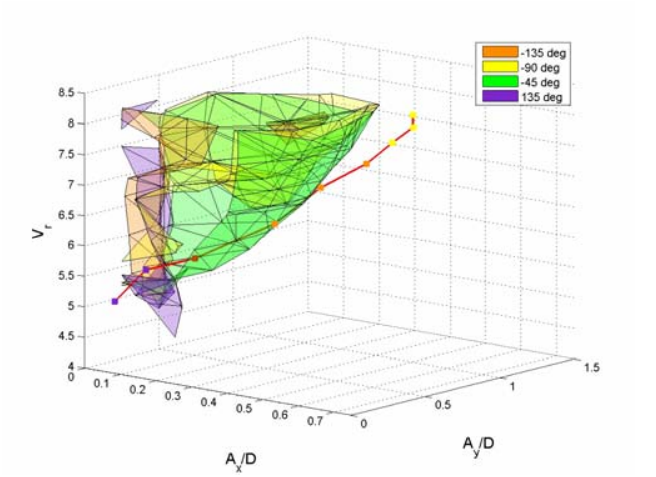

Fig. 3: View 1 of forced vibration surfaces of zero average power coefficients with curve from observed motions of Jauvtis and Williamson (2004). Colors indicate the zero average power surfaces for fixed phase. The combined surfaces bound the observed motions from free vibrations.

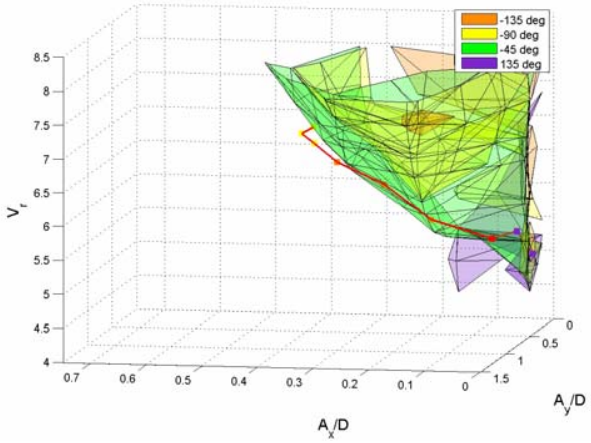

Fig. 4: View 2 of forced vibration surfaces of zero average power coefficients with curve from observed motions of Jauvtis and Williamson (2004). Colors indicate the zero average power surfaces for fixed phase. The combined surfaces bound the observed motions from free vibrations.

Figs. 5 and 6 show similar average power surfaces with slightly different phases between motions. A line of data points indicates the free vibration motions of Dahl et al (2006) with a natural frequency ratio of 1.9. Again, the free vibration values follow closely along the boundary formed by the surfaces; however, the path through the parameter space is much different than that observed by Jauvtis and Williamson (2004). The experiments of Dahl et al (2006) had unequal masses in the in-line and cross-flow directions and the natural frequency ratio was 1.9. In both cases, the particular path through the data space describes a valid set of free vibration motions and the large variety of motion combinations defined by the zero average power surfaces establishes how these various different paths are possible. This signifies that surfaces of average power may be a useful condition for predicting the steady-state free vibration of an elastically mounted cylinder given additional constraints.

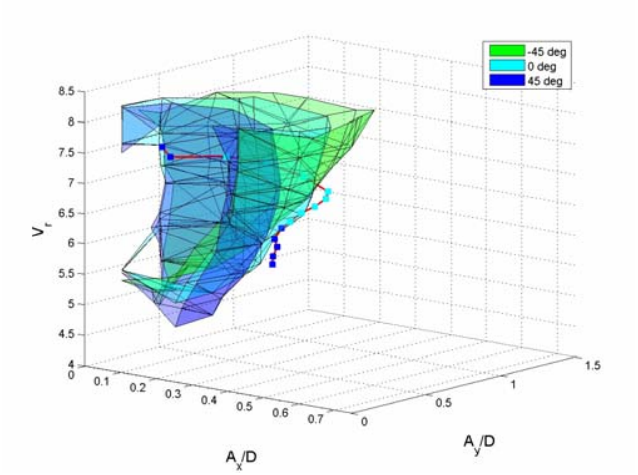

Fig. 5: View 1 of forced vibration surfaces of zero average power coefficients with curve from observed motions of Dahl et al (2006). Colors indicate the zero average power surfaces for fixed phase. The combined surfaces bound the observed motions from free vibrations.

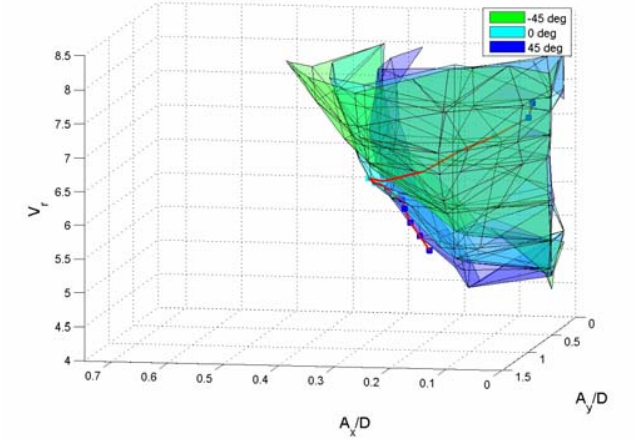

Fig. 6: View 2 of forced vibration surfaces of zero average power coefficients with curve from observed motions of Dahl et al (2006). Colors indicate the zero average power surfaces for fixed phase. The combined surfaces bound the observed motions from free vibrations.

Third Harmonic Lift Coefficient

Large magnitude third harmonic forces observed from vortex-induced vibrations occur with combined in-line and cross-flow motion of the cylinder. Figs. 7-9 show the magnitude of third harmonic lift coefficient observed with varied in-line motion, cross-flow motion, and phase between motions for three fixed reduced velocities, 4.5, 6.5, and 8. The colored surfaces indicate different magnitudes of the third harmonic lift coefficient. Third harmonic portion of lift is reported as the peak value, calculated by the square root of the integral of the lift coefficient power spectral density, integrated over the region of the third harmonic frequency.

At the lowest reduced velocity shown, V_r = 4.5, third harmonic magnitudes do not appear to be largely affected by the phase between in-line and cross-flow motions. This is indicated by the nearly constant values of third harmonic lift coefficient as one follows a vertical line through Fig. 7. At this reduced velocity, large magnitude forces occur with high dependence on both in-line and cross-flow motions as indicated by the force iso-surfaces being aligned at an angle though the plane formed by in-line and cross-flow motion. Free vibrations at this reduced velocity typically occur with fairly small in-line and cross-flow amplitudes ($A_y/D < 0.5$, $A_x/D < 0.2$), hence one would expect fairly small magnitudes of third harmonic forces in free vibrations at this reduced velocity.

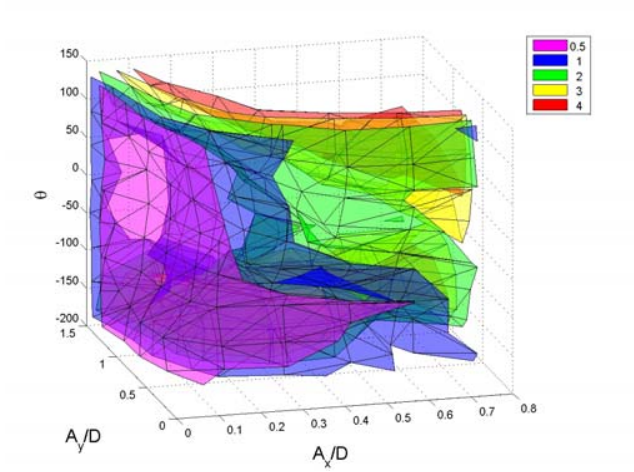

Fig. 7: Iso-surfaces of third harmonic lift coefficient magnitude with fixed V_r = 4.5.

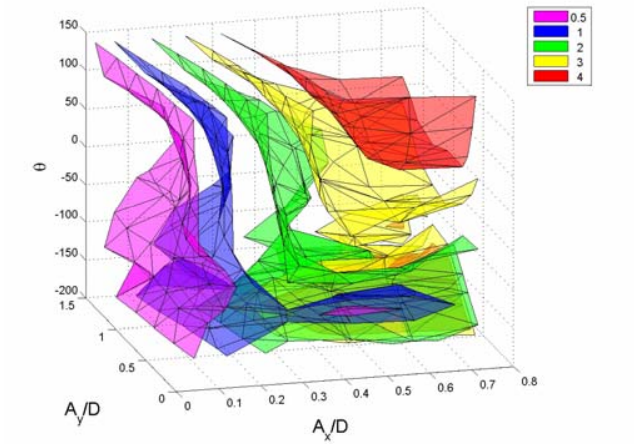

Fig. 8: Iso-surfaces of third harmonic lift coefficient magnitude with fixed V_r = 6.5. As V_r increases, fixed values of third harmonic magnitude become more aligned with fixed A_x/D.

As reduced velocity increases, the iso-surfaces of the third harmonic component of lift coefficient become more aligned with in-line motions; hence, becoming less dependent on cross-flow motions of the cylinder. This is apparent in Fig. 8, where the same magnitude surfaces have rotated such that lower amplitude cross-flow motions experience nearly the same magnitude third harmonic force as higher amplitude motions (with low amplitude in-line motions). This phenomenon is more clearly shown by fixing the phase of motion such that we only view a cross-section of these iso-surfaces. Figs. 10-12 show contours of third harmonic lift coefficient for the same fixed reduced velocities with fixed phase θ = 0 degrees. One can see that at a reduced velocity of 4.5, contours are generally aligned with a negative slope, while at reduced velocities of 6.5 and 8, the contours have shifted to a positive slope.

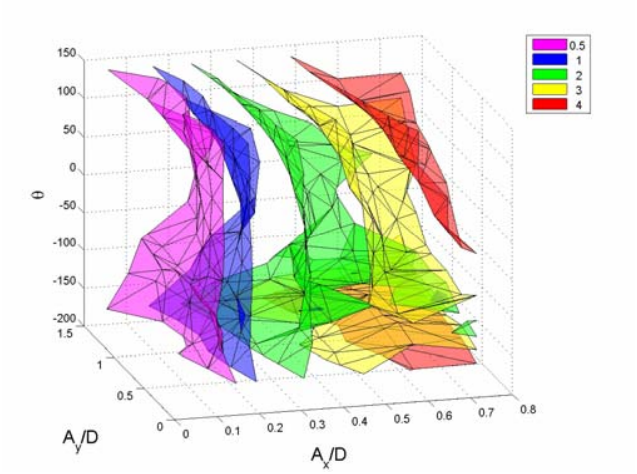

Fig. 9: Iso-surfaces of third harmonic lift coefficient magnitude with fixed V_r = 8. As V_r increases, fixed values of third harmonic magnitude become more aligned with fixed A_x/D; at the highest reduced, third harmonic magnitude is nearly completely a function of in-line motion.

With combined cross-flow and in-line motion of the cylinder at a reduced velocity of 6.5, in-line amplitudes are typically less than 0.4, in which case, third harmonic lift coefficient magnitudes are less than 2. This magnitude of force is still very significant and if properly phased with a first harmonic portion of lift coefficient, peak magnitudes of the total lift coefficient can become very large, with peak magnitudes near 5. Large peak magnitudes in lift lead to increased material stresses in physical risers and reduction in the fatigue life of the structure. A larger dependence on phase between motions is apparent in the local curvature of surfaces in Fig. 8. For relatively moderate amplitude cross-flow motion ($A_y/D < 0.75$), moderate in-line motion ($A_x/D < 0.3$), a local maximum in third harmonic magnitude occurs with a phase of 0 degrees compared with other phases at this reduced velocity; a local minimum occurs with a phase of -135 degrees. A phase of 0 degrees corresponds to a figure eight motion with the cylinder moving upstream at the extreme cross-flow motions. This particular motion has been shown to occur when a freely vibrating cylinder is excited with dual resonance, and typically results in a dominant third harmonic forcing function (Dahl et al 2007). The local minimum occurs with a figure eight motion curved slightly downstream, where the cylinder moves in the opposite direction of motion.

At the highest reduced velocity shown, V_r = 8, the iso-surfaces of third harmonic lift coefficient have completely changed orientation within the parameter space. At the lowest reduced velocity, large third harmonic forces were associated with large cross-flow motions. At the highest reduced velocity, third harmonic forces tend be larger with lower cross-flow amplitude, for a given in-line amplitude of motion. Again, this phenomenon is apparent in the contours of Figs. 10-12. A high dependence on the in-line motion of the cylinder is still apparent and local dependence on the phase of motion is apparent as well.

The third harmonic portion of lift occurs due to the presence of vortices in the wake of the cylinder. The relative motion of these vortices with respect to the cylinder motions determines the magnitude and phasing of forces exerted on the cylinder. The phase relationship between the different force components can largely affect the peak magnitudes observed for the total lift coefficient. The particular phasing between the first harmonic component of lift force and the third harmonic component of lift force can drastically change the observed peak magnitude of lift coefficients, since odd harmonics can amplify or diminish the peak amplitude of forces depending on the phase relationship between the harmonic components of the force. The third harmonic forces in these experiments can take on very large amplitude values, particularly for large amplitude forced motions in both in-line and cross-flow directions.

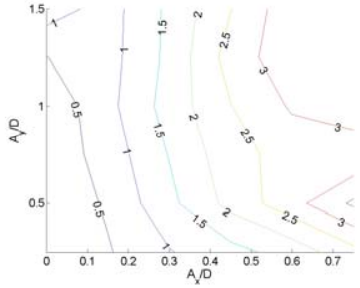

Fig. 10: Contours of third harmonic lift coefficient magnitude for V_r = 4.5 and θ = 0 degrees. Contours show third harmonic lift is primarily dependent on in-line cylinder motions with higher magnitude third harmonic lift occurring at higher cross-flow amplitudes.

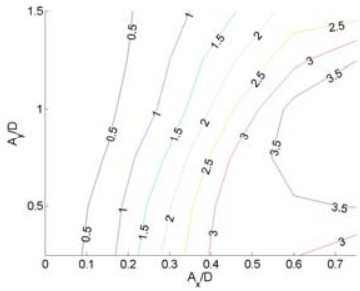

Fig. 11: Contours of third harmonic lift coefficient magnitude for V_r = 6.5 and θ = 0 degrees. Contours show third harmonic lift is primarily dependent on in-line cylinder motions with higher magnitude third harmonic lift occurring at lower cross-flow amplitudes.

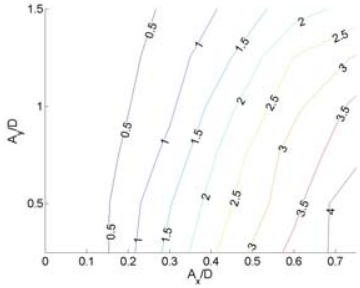

Fig. 12: Contours of third harmonic lift coefficient magnitude for V_r = 8 and θ = 0 degrees. Contours show third harmonic lift is primarily dependent on in-line cylinder motions with higher magnitude third harmonic lift occurring at lower cross-flow amplitudes.

PREDICTION OF FREE VIBRATIONS

Predicting the motions of an elastically mounted, rigid cylinder acts as a stepping stone towards predicting the motions of a fully flexible riser. In the previous section, it was seen that free vibrations tend to lie directly along the surfaces of zero average power from forced vibration experiments. How does one determine exactly where on these surfaces a particular free vibration exists? What additional assumptions are

necessary to be able to predict the motions of an elastically mounted, rigid cylinder?

Dual Lock-in Assumption

Under conditions of lock-in, the fluid wake behind the cylinder interacts with the structural characteristics of the system such that the cylinder resonates at an effective natural frequency. The excitation frequency is defined by Sarpkaya (2004) as in equation 10, where f_{ex} is the excitation frequency, k is the spring constant, m is the structural mass, and m_a is the effective added mass.

$$f_{ex} = \frac{1}{2\pi}\sqrt{\frac{k}{m+m_a}} \tag{10}$$

When the excitation frequency is equal to the oscillation frequency of the system, lock-in occurs. In free vibration experiments, it is possible for lock-in to occur in both the in-line direction and cross-flow direction if the effective added mass associated with each direction allows for the in-line excitation frequency to be twice the cross-flow excitation frequency. Fig. 13 shows the ratio of in-line excitation frequency to cross-flow excitation frequency for various free vibration cases from Dahl et al (2006) with different nominal natural frequency ratios. In each case, the excitation frequency ratio is driven towards a value of 2, indicating that dual lock-in is possible.

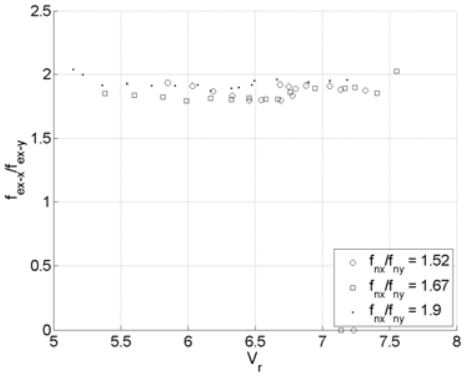

Fig. 13: Ratio of in-line excitation frequency and cross-flow excitation frequency. Dual lock-in occurs when this ratio equals 2 and is equal to the oscillation frequency ratio.

Predicted Free Vibrations

If one assumes that dual lock-in occurs, the frequencies of oscillation are known, given a particular flow velocity and reduced velocity. In this case, equation 10 can be used to solve for the effective added mass necessary for this assumption to be true. For a given reduced velocity, the values of zero average power, effective in-line added mass, and effective cross-flow added mass are known values. In the context of the forced vibration database, each of these values form a surface within the in-line motion, cross-flow motion, and phase between motions parameter space (for fixed reduced velocity). The intersection of these surfaces defines the point where all of these values exist within the database and the particular motions associated with that intersection point are the predicted free vibration motions. Prediction of the free vibration then involves merely finding the appropriate database value where average power is zero, in-line added mass is equal to the lock-in value at the particular reduced velocity, and cross-flow added mass is equal to the lock-in value at the particular reduced velocity.

Figs. 14-16 show the comparison of predicted motions from forced cylinder motions compared with the observed motions of an elastically mounted, rigid cylinder from Dahl et al (2006). The predicted motions are fairly good at representing the general trend of the free vibration motions, while also predicting relatively close values for both in-line and cross-flow motion amplitudes and the phase between the motions. The largest error occurs in the prediction of cross-flow amplitudes at reduced velocities near 7.

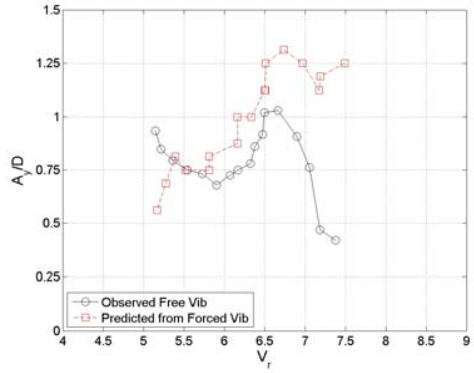

Fig. 14: Comparison of predicted cross-flow amplitudes with observed free vibrations for elastically mounted, rigid cylinder with f_{nx}/f_{ny} = 1.9.

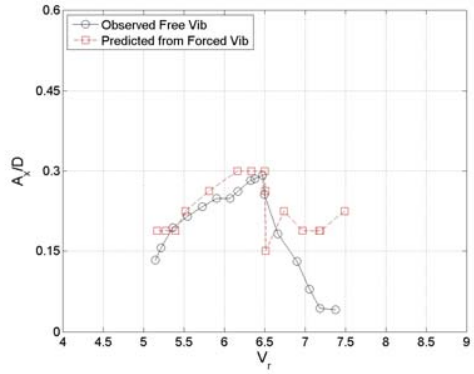

Fig. 15: Comparison of predicted in-line amplitudes with observed free vibrations for elastically mounted, rigid cylinder with f_{nx}/f_{ny} = 1.9.

Prediction of the cross-flow amplitudes in Fig. 14 shows the double peak that occurs as a function of reduced velocity. Errors are less than 20% of the free vibration value, except at reduced velocities above 7. Prediction of the in-line amplitudes and phase between motions are very good, again with slight discrepancies occurring at the highest reduced velocities. The discrepancy at higher reduced velocities occurs where the dual lock-in assumption is no longer valid, and the free vibration system is outside of the excitation region. A more detailed prediction method to balance the forces in the equations of motion is necessary to properly predict motions in this region. The grid spacing on Figs. 14-16 indicate the sparseness of the test matrix and prediction errors are generally contained to within one grid spacing of the observed free vibration. In order to generate sub-grid resolution of predicted amplitudes, it is necessary to interpolate the observed force values of the test matrix. The grid points of the test matrix and limited resolution from interpolation results in prediction curves that are not consistently smooth across the reduced velocity range.

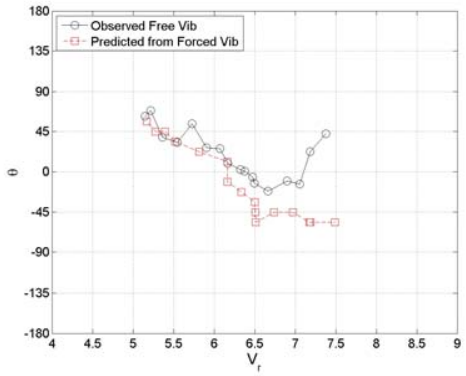

Fig. 16: Comparison of predicted phase between in-line and cross-flow motion with observed free vibrations for elastically mounted, rigid cylinder with $f_{nx}/f_{ny} = 1.9$.

DISCUSSION

The prediction of free vibration motions in the in-line and cross-flow directions is a first step towards predicting the motions and forces associated with the vibration of a long riser in the ocean. In this simplified case, knowing the particular motions of the rigid cylinder also directly gives force measurements on the structure; thus, magnitudes of first and third harmonic forces and the phase relation of these forces are known quantities if the motions are known for the given Reynolds number.

Prediction of the elastically mounted cylinder motions is very good considering the sparseness of the test matrix and the simplicity of the assumptions made in the prediction. In reality, it is not necessary for the cylinder to undergo lock-in in both the in-line and cross-flow directions since energy can easily transfer from one direction to the other in order to drive the motions of the cylinder at some other forced frequency. In this case, this prediction method breaks down. The frequency ratio between in-line and cross-flow excitation frequencies will not be two, but rather some other value dependent on the particular flow conditions. One can see from Fig. 13 that the excitation frequency ratio for the lower nominal natural frequency ratios may be nearer to 1.9 than 2. Additionally, this value is a function of reduced velocity and can change depending on the particular reduced velocity. Improved predictions exist if this value is tuned to the particular flow conditions.

Although improved predictions may be made by tuning the excitation frequency ratio, this assumption requires knowledge about the excitation frequencies a priori. If the excitation frequencies are known beforehand, then the cylinder motions are known beforehand, making the prediction obsolete. The assumption that the excitation frequency ratio must equal two allows a prediction to be made without prior knowledge of free vibration motions. This assumption works best when the nominal natural frequency ratio is near two. As mentioned in the introduction, long string-like risers cannot avoid this condition as the nominal natural frequency ratio along the length can always take a value of two.

Complete measurements of the forces associated with vortex-induced vibrations in combined cross-flow and in-line motion are necessary for truly predicting the fatigue life of long risers. It was shown in Dahl et al (2007) through a simple example that the added material stresses due to third harmonic lift forces may lead to a reduction in riser fatigue life. More detailed studies of true fatigue life reduction are necessary to truly understand the effect of large amplitude third harmonic forces on fatigue life.

Although third harmonic forces have been shown to be fairly large in magnitude, the phase relation between these forces and the first harmonic force is important as well, since the peak magnitude of lift forces will be affected by this phase relationship.

CONCLUSIONS

We have presented a study of the forced motions of a rigid cylinder in combined cross-flow and in-line motion. This coupled motion results in large amplitude third harmonic forces in addition to traditionally observed forces that occur near the frequency of vortex shedding. The third harmonic forces have been shown to be largely dependent on the in-line motion of the cylinder and the peak magnitude of the lift force coefficient associated with the third harmonic can take on values near two for typical free vibration motions. The sparse test matrix of cylinder motions also provides a basis for predicting the free vibration motions of a cylinder in combined cross-flow and in-line motion. The simplifying assumptions that lock-in must occur in both the in-line and cross-flow direction results in successful prediction of the free vibration motions of a cylinder. Further study is necessary to truly understand the detrimental effect of large third harmonic forces on long, flexible marine risers and to extend the prediction of motions to a fully flexible marine riser.

REFERENCES

Bearman, PW (1984). "Vortex Shedding from Oscillating Bluff Bodies," *Ann Rev Fluid Mech*, Vol 16, pp 195-222.

Dahl, JM, Hover, FS, and Triantafyllou, MS (2006). "Two-Degree-of-Freedom Vortex-Induced-Vibrations Using a Force Assisted Apparatus," *J Fluids Struct*, Vol 22, pp 807-818.

Dahl, JM, Hover, FS, Triantafyllou, MS, Dong, S, and Karniadakis, GE (2007). "Resonant Vibrations of Bluff Bodies Cause Multi-vortex Shedding," *Phys Rev Lett*, Vol 99, no 144503.

Jauvtis, N, and Williamson, CHK (2004). "The Effect of Two Degrees of Freedom on Vortex-Induced Vibration at Low Mass and Damping," *J Fluid Mech*, Vol 509, pp 23-62.

Jeon, D, and Gharib, M (2001). "On Circular Cylinders Undergoing Two Degree of Freedom Forced Motions," *J Fluids Struct*, Vol 15, pp 533-541.

Khalak, A, and Williamson, CHK (1996). "Dynamics of a Hydroelastic Cylinder with Very Low Mass and Damping," *J Fluids Struct*, Vol 10, pp 455-472.

Sarpkaya, T (1979). "Vortex Induced Oscillations," *J Applied Mech*, Vol 46, pp 241-258.

Sarpkaya, T (1995). "Hydrodynamic Damping, Flow-Induced Oscillations, and Biharmonic Response," *ASME J Offshore Mech and Arctic Eng*, Vol 117, pp 232-238.

Sarpkaya, T (2004). "A Critical Review of the Intrinsic Nature of Vortex-Induced Vibrations," *J Fluids Struct*, Vol 19, pp 389-447.

Williamson, CHK, and Govardhan, R (2004). "Vortex-Induced Vibrations," *Ann Rev Fluid Mech*, Vol 36, pp 413-455.